Biochem. J. (2012) **441**, 803–812 (Printed in Great Britain) doi:10.1042/BJ20111474

online data

## SUPPLEMENTARY ONLINE DATA

# The multifunctional poly(A)-binding protein (PABP) 1 is subject to extensive dynamic post-translational modification, which molecular modelling suggests plays an important role in co-ordinating its activities

Matthew BROOK*†[1], Lora McCRACKEN*[2], James P. REDDINGTON†, Zhi-Liang LU*[3], Nicholas A. MORRICE‡[4] and Nicola K. GRAY*†

*MRC Centre for Reproductive Health/MRC Human Reproductive Sciences Unit, Queen's Medical Research Institute, University of Edinburgh, 47 Little France Crescent, Edinburgh EH16 4TJ, Scotland, U.K., †MRC Human Genetics Unit, Institute of Genetics and Molecular Medicine, Western General Hospital, Crewe Road, Edinburgh EH4 2XU, Scotland, U.K., and ‡MRC Protein Phosphorylation Unit, The Sir James Black Centre, College of Life Sciences, University of Dundee, Dow Street, Dundee DD1 5EH, Scotland, U.K.

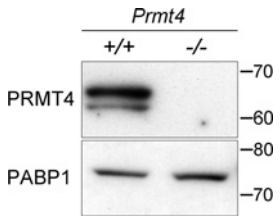


**Figure S1 Confirmation of the PRMT4-deficient status of *Prmt4*$^{-/-}$ MEFs**

Lysates from *Prmt4*$^{+/+}$ and *Prmt4*$^{-/-}$ MEFs were immunoblotted to detect PRMT4. As expected, PRMT4 is readily detectable in *Prmt4*$^{+/+}$ MEFs, but not in *Prmt4*$^{-/-}$ MEFs. PABP1 is utilized as a loading control. Molecular mass in kDa is indicated.

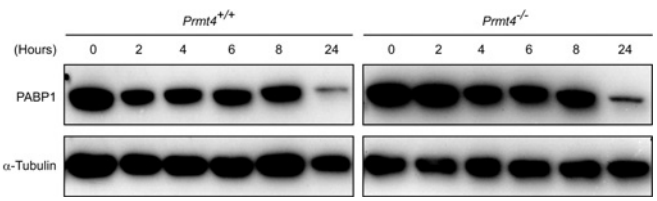


**Figure S2 Comparison of PABP1 protein stability in *Prmt4*$^{+/+}$ and *Prmt4*$^{-/-}$ MEFs**

Protein synthesis was inhibited by the addition of 15 $\mu$g/ml cycloheximide and cell extracts were prepared either immediately ($t = 0$) or after the indicated times. Equal amounts of protein were immunoblotted to determine PABP1 levels and $\alpha$-tubulin was utilized as a loading control. In both *Prmt4*$^{+/+}$ and *Prmt4*$^{-/-}$ MEFs, PABP1 is stable for at least 8 h after inhibition of its synthesis and remains weakly detectable after 24 h, indicating no significant role for PRMT4-dependent methylation in regulating PABP1 protein stability.

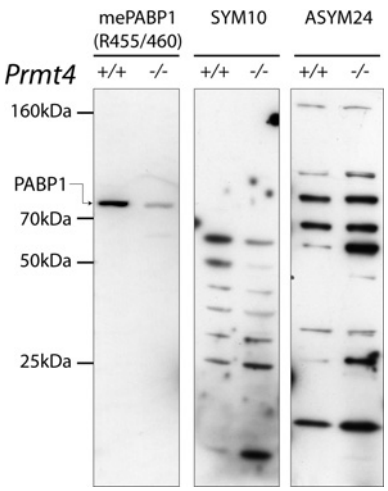


**Figure S3 Detection of methylarginine-containing proteins in *Prmt4*$^{+/+}$ and *Prmt4*$^{-/-}$ MEF lysates**

Input lysates from immunoprecipitations in Figure 2(A) of the main text were Western blotted with the anti-(methyl-PABP1), SYM10 and ASYM24 anti-(methyl-arginine) antibodies. The specific anti-(methyl-PABP1) antibody detects modified PABP1 in input lysates and the reduction in PABP1 methylation in *Prmt4*$^{-/-}$ MEFs (left-hand panel). The SYM10 and ASYM24 antibodies do not detect PABP1 in input lysates, although ASYM24 detects PABP1 in immunoprecipitates (Figure 2A of the main text). Both antibodies detect numerous other methylated antigens [1], therefore the lack of a PABP1 signal using the SYM10 antibody in Figure 2(A) of the main text is due to the absence of symmetrically dimethylated arginine residues in PABP1. Molecular mass in kDa is indicated.

[1] To whom correspondence should be addressed (email matt.brook@ed.ac.uk).
[2] Present address: Tissues and Cells Directorate, Scottish National Blood Transfusion Service, 21 Ellen's Glen Road, Edinburgh EH17 7QT, Scotland, U.K.
[3] Present address: Department of Biological Sciences, Xi'an Jiaotong-Liverpool University, Suzhou Dushu Lake Higher Education Town, China 215123
[4] Present address: The Beatson Institute for Cancer Research, Garscube Estate, Switchback Road, Bearsden, Glasgow G61 1BD, Scotland, U.K.

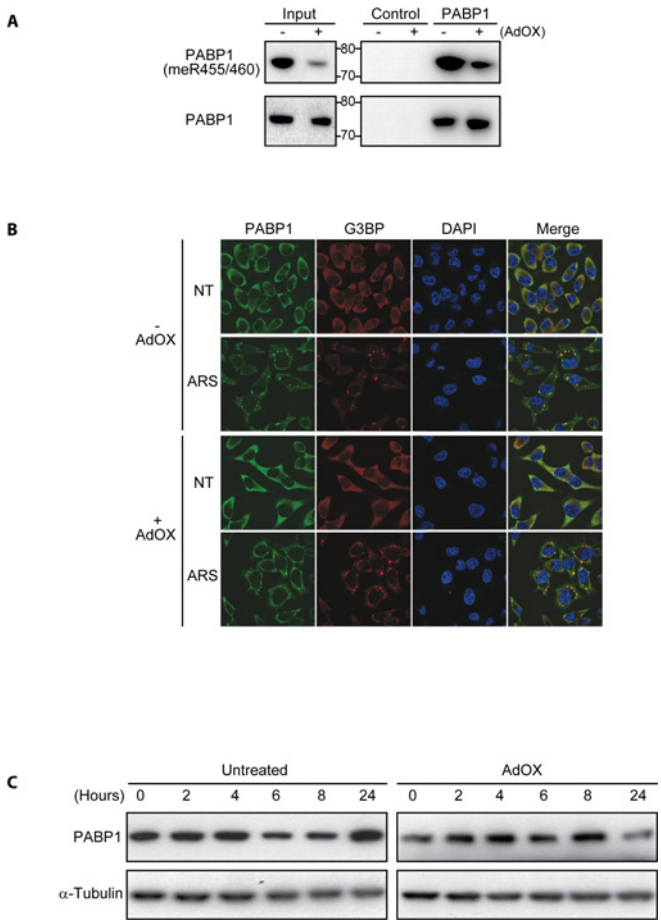


**Figure S4 Effects of AdOX treatment of PABP1 in HeLa cells**

(**A**) The inhibitory effects of AdOX treatment were verified by immunoblotting cell extracts (input, left-hand panel) and immunoprecipitated PABP1 using anti-(dimethyl-Arg$^{455}$/Arg$^{460}$-PABP1) or anti-PABP1 antibodies. Control immunoprecipitations were performed using purified rabbit IgG (right-hand panel). (**B**) AdOX treated ( + AdOX) or untreated cells ( − AdOX) cells either received no further treatment (NT) or were treated with 500 $\mu$M sodium arsenite (ARS), and PABP1 (green) intracellular distribution was visualized by confocal immunofluorescence microscopy. SG formation was marked by detection of G3BP (red) and DNA was visualized by DAPI staining (blue). This revealed that the normal nucleocytoplasmic distribution of PABP1 was unaffected by AdOX treatment, and neither were SG formation or recruitment of PABP1 to SGs. (**C**) Effect of AdOX treatment on PABP1 protein stability. Protein synthesis was inhibited by the addition of 15 $\mu$g/ml cycloheximide and cell extracts were prepared either immediately ($t = 0$) or after the indicated times. Equal amounts of protein were immunoblotted to determine PABP1 levels and $\alpha$-tubulin was detected as a loading control. This showed that PABP1 was highly stable in HeLa cells and that AdOX treatment did not result in a reproducible effect on PABP1 protein stability.

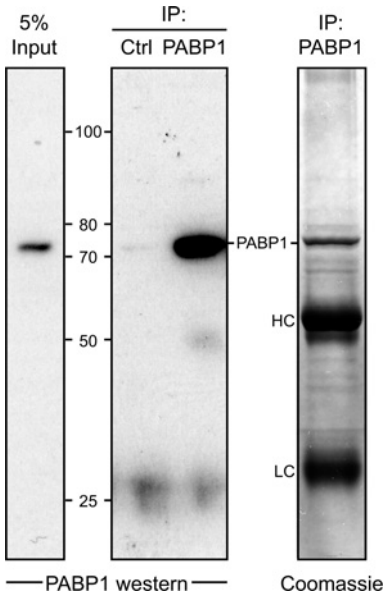


**Figure S5 Specific immunoprecipitation of PABP1 for detection of methylated arginine residues and for MS**

PABP1 was immunoprecipitated from cell lysate (input, left-hand panel) using anti-PABP1 or normal rabbit IgG (Ctrl) antibodies. Immunoprecipitates (IP) were validated for specificity by Western blotting for PABP1 (middle panel). For MS studies, immunoprecipitated PABP1 was visualized by GelCode Coomassie Blue staining and the ~73 kDa PABP1 band was excized for analysis. A representative immunoprecipitation from *Prmt4*$^{+/+}$ MEFs is shown. HC, heavy chain, LC, light chain. Molecular mass in kDa is indicated.

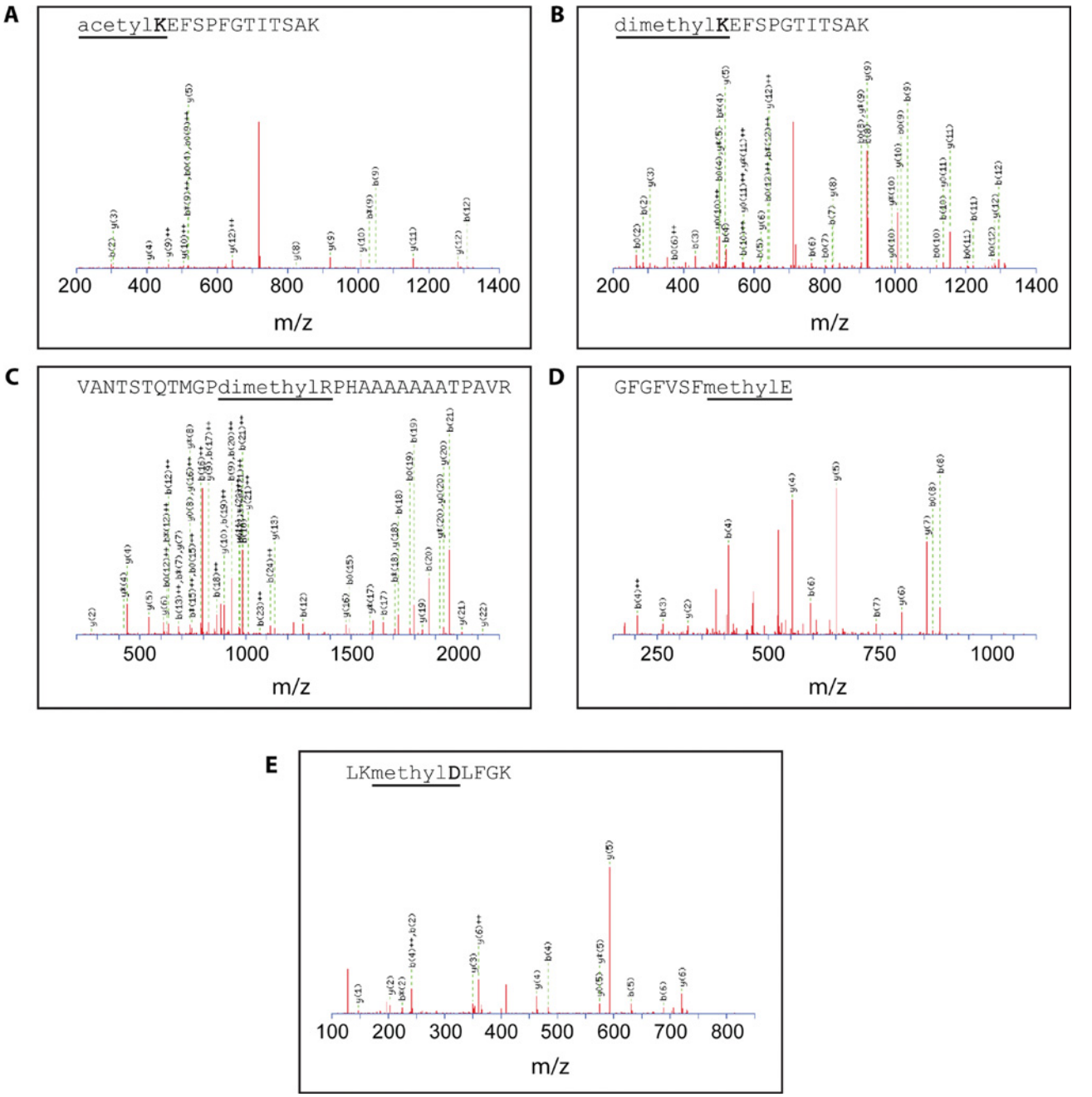


**Figure S6 Representative MS/MS spectra for post-translationally modified peptides identified in human PABP1**

MS/MS spectra acquired on an LTQ-orbitrap LC-MS system were searched using Mascot version 2.2 allowing for various PTMs of arginine, lysine, serine, threonine, tyrosine, aspartate and glutamate residues. MS/MS spectra matching selected PABP1 tryptic peptides, each with an ion score greater than 38 (See Table 1 of the main text), were assigned and contained the following PTMs (evidence from ion series) (**A**) acetylated Lys$^{312}$ ($b2$ ion = $m/z$ 300.15; acetyl-KE), (**B**) dimethylated Lys$^{312}$ ($b2 = m/z$ 286.1; dimethyl-KE), (**C**) dimethylated Arg$^{493}$, (**D**) methylated Glu$^{239}$ ($b8 - b7$ ion = 143 Da; methylglutamate), (**E**) methylated Asp$^{209}$ ($y5 - y4 = 143$ Da; methylaspartate).

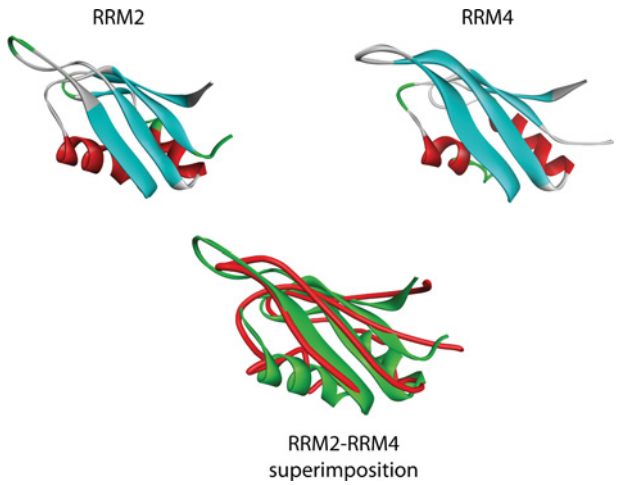


**Figure S7 Modelling of human PABP1 RRM4**

The structure of human PABP1 RRM4 (top right-hand panel) was modelled based on the structure of human tPABP RRM4 (PDB code 2D9P). The predicted structure of RRM4 was compared with the crystal structure of human PABP1 RRM2 (top left-hand panel) (PDB code 1CVJ) by superimposition (bottom; green, RRM2; red, RRM4). Ribbon models of the two separate RRMs are shown colour-coded for secondary structure type (cyan, $\beta$-sheet; red, $\alpha$-helix; white, coil; green, turn). This shows that the predicted structure of human PABP1 RRM4 is highly similar to the solved structure of human PABP1 RRM2 and validates the use of the RRM2 structure for predicting the spatial position of modified residues in RRM4.

**Table S1 Table of PTMs identified in mouse PABP1**

Peptides identified to contain modified residues (bold) are shown. In each case the highest recorded Mascot score for the modified ( + ) peptide is given. Where the modified peptide was not detected, the presence of the unmodified ( − ) peptide is recorded. All spectra from putative modified peptides were subject to manual verification. Blank domain column entries indicate that the residue is situated within the respective inter-RRM spacer region. PTMs not detected in human PABP1 are in italics. *, ion scored below Mascot cut-off score of 20 but was manually verified.

| Domain | Amino acid | Modification | Peptide | Mascot score | |
|---|---|---|---|---|---|
| | | | | *Prmt4*$^{+/+}$ MEFs | *Prmt4*$^{-/-}$ MEFs |
| RRM1 | *Glu*$^{66}$ | Methylation | SLGYAYVNFQQPADA**E**R | + (93) | − (88) |
| RRM1–RRM2 spacer region | Lys$^{95}$ | Acetylation | **K**SGVGNIFIK | + (29) | + (29) |
| RRM2 | *Glu*$^{134}$ | Methylation | VVCD**E**NGSK | + (58) | − (22) |
| | *Glu*$^{149}$ | Methylation | GYGFVHFETQ**E**AAER | + (79) | − (96) |
| RRM2–RRM3 spacer region | Glu$^{180}$ | Methylation | **E**A**E**LGAR | + (26) | + (21) |
| | Glu$^{182}$ | Methylation | **E**A**E**LGAR | + (26) | + (21) |
| | Lys$^{188}$ | Acetylation | A**K**EFTNVYIK | + (28) | + (29) |
| RRM3 | *Glu*$^{205}$ | Methylation | NFGEDMDD**E**R | + (51) | + (47) |
| | Glu$^{239}$ | Methylation | GFGFVSF**E**R | + (50) | + (58) |
| RRM4 | Lys$^{299}$ | Methylation | YQGVNLYV**K** | + (44) | + (46) |
| | *Glu*$^{308}$ | Methylation | NLDDGIDD**E**R | + (60) | + (58) |
| | Lys$^{312}$ | Acetylation | EFSPFGTITSAK | + (65) | + (62) |
| | Lys$^{312}$ | Dimethylation | **K**EFSPFGTITSAK | − (81) | + (85) |
| | *Glu*$^{345}$ | Methylation | GFGFVCFSSPE**E**ATK | + (55) | + (22) |
| | Lys$^{361}$ | Acetylation | IVAT**K**PLYVALAQR | + (22) | + (25) |
| | Lys$^{361}$ | Dimethylation | IVAT**K**PLYVALAQR | − (87) | + (99) |
| Proline-rich linker region | *Arg*$^{432}$ | Methylation | AAYYPPSQIAQL**R**PSPR | + (17)* | + (39) |
| | Arg$^{493}$ | Dimethylation | VANTSTQTMGP**R**PAAAAAAATPAVR | + (74) | + (80) |
| | Arg$^{493}$/Arg$^{506}$ | Dimethylation, methylation | VANTSTQTMGP**R**PAAAAAAATPAV**R** | + (52) | − (80) |
| PABC/MLLE | *Glu*$^{564}$ | Methylation | QMLG**E**R | + (24) | − (30) |
| | Lys$^{606}$ | Acetylation | S**K**VDEAVAVLQAHQAK | + (26) | + (31) |
| | Lys$^{606}$ | Dimethylation | S**K**VDEAVAVLQAHQAK | − (90) | + (42) |

## REFERENCE

1 Boisvert, F. M., Côté, J., Boulanger, M. C. and Richard, S. (2003) A proteomic analysis of arginine-methylated protein complexes. Mol. Cell. Proteomics **2**, 1319–1330

Received 15 August 2011/13 October 2011; accepted 18 October 2011
Published as BJ Immediate Publication 18 October 2011, doi:10.1042/BJ20111474